ASSESSING AIR POLLUTANT EMISSIONS IN THE AFTERMATH OF THE 2021 FOREST FIRES IN MARMARIS AND MANAVGAT, TÜRKİYE: INSIGHTS FROM SATELLITE-BASED MONITORING

C. Serifoglu Yilmaz

Karadeniz Technical University, Department of Geomatics Engineering, 61080 Trabzon, Türkiye - cigdemserifoglu@ktu.edu.tr

KEY WORDS: Forest Fire, Google Earth Engine, TROPOMI, Sentinel-5P, Burn Severity, Remote Sensing.

ABSTRACT:

In recent years, the occurrence of forest fires has become almost inevitable worldwide due to the severe impact of climate change. Consequently, it is imperative to examine the consequences of these fires, pinpoint the affected areas, and take required measures following post-fire incidents. With the advent of modern remote sensing satellites, which allow for the rapid monitoring of vast expanses, they offer a valuable data source for addressing such emergency scenarios. Therefore, the main objective of this study is to evaluate the extent of air pollutant gas emissions resulting from the forest fires that occurred in Marmaris and Manavgat, Türkiye, in the summer of 2021. To this aim, using the data obtained from the TROPOspheric Monitoring Instrument (TROPOMI) sensor onboard the Sentinel-5P satellite, the amount of major air pollutants nitrogen dioxide (NO_2), carbon monoxide (CO) and aerosol were investigated after the forest fires considering three different non-fire time periods. The findings of the experiments indicated that in Manavgat, there was a substantial rise in NO_2 and average CO levels by 260.43% and 107.07%, respectively, when compared to the 10-day period preceding the forest fire event. Similarly, in Marmaris, there was an increase of 203.63% in NO_2 levels and a 102.47% rise in average CO levels during the same period. Positive absorbing aerosol index (AAI) values were also observed during the events, which means that the amount of UV-absorbing aerosols increased due to the fire. The differenced Normalized Burn Ratio (dNBR) maps derived from the Sentinel-2 MSI imagery were also used to investigate the severity of the forest fires, and to observe the relationship between the fire severity level and the air pollutants investigated.

1. INTRODUCTION

Trees and forests play a crucial role in addressing climate change. They house a substantial amount of carbon, totaling 662 billion tonnes, surpassing more than half of the global carbon stored in both soil and vegetation. They encompass 31% of the Earth's land area, equivalent to 4.06 billion hectares, yet this expanse is decreasing. Deforestation resulted in the loss of 420 million hectares of forest between 1990 and 2020 (FAO, 2022).

Wildfires pose a substantial natural threat annually, resulting in deforestation, the release of carbon emissions, and the loss of human and animal lives (Shmuel and Heifetz, 2022). Climate change is having an impact on wildfire patterns and behavior in a number of ways, even though wildfires are a natural element of many ecosystems and can have a variety of causes, including human activity. For instance, wildfires emit large amounts of carbon dioxide (CO_2) into the atmosphere. As a greenhouse gas, CO_2 contributes to the warming of the Earth's climate. With this warming, increased wildfires release more CO_2, contributing further to climate change; this may, in turn, influence future wildfire patterns. According to study conducted by Randerson et al. (2012), the increasing frequency of wildfires is leading to a rise in CO_2 emissions, contributing to the acceleration of global warming, which can be considered as the long-term effects of forest fires.

The immediate impacts of forest fires involve the deterioration of air quality due to the substantial release of gaseous pollutants, particulate matter (PM), and aerosols into the atmosphere (Brey et al., 2018; Butt et al., 2020; Goparaju et al., 2023). These pollutants can be measured by ground measurement stations that assess local air quality; however, the type of pollutants measured by stations can vary from station to station, and some regions lack adequate number of stations. The tropospheric monitoring sensor (TROPOMI - Tropospheric Monitoring Instrument) on the Sentinel-5 Precursor (Sentinel-5P) satellite (Veefkind et al., 2012), which is part of the Copernicus program, provides a crucial service for understanding the quantity and spatio-temporal distribution of air pollution.

Air pollution was previously studied by scientists using images provided by satellites such as Landsat (Tanré et al., 1988; Retalis, 1999; Wald, 1999; Lim et al., 2004; Gündüz, 2018), SPOT (Sifakis and Deschamps, 1992), Moderate-Resolution Imaging Spectroradiometer (MODIS) (Gupta et al., 2006; Harbula and Kopacková, 2011); however, with the launch of the Sentinel-5P satellite in 2017, it can be observed that research in this field has become more practical and has increased. Tariq et al. (2020) evaluated air quality parameters in Türkiye and its surroundings between 2018 and 2021. They examined aerosol optical depth (AOD), absorbing aerosol index (AAI), nitrogen dioxide (NO_2), ozone (O_3), formaldehyde (HCHO), and carbon monoxide (CO) concentrations obtained from the Sentinel-5P satellite. Ghasempour et al. (2021) examined the impact of COVID-19 quarantine on air pollution in Türkiye. The analysis, conducted using Sentinel-5P TROPOMI data, identified a notable reduction in NO_2 and AOD during the quarantine, while sulfur dioxide (SO_2) remained unchanged or exhibited moderately higher concentrations in certain regions. The study concluded with strong evidence that human activities contribute significantly to air pollution and that the quarantine improved air quality. Magro et al. (2021) conducted a study evaluating the efficacy of Sentinel 5-P TROPOMI in monitoring CO and methane (CH_4) levels during severe fire incidents in Portugal. The monitoring of both gases indicated that CO measurements exhibit an obvious trend,

identifiable patterns, and a distinct distribution, aligning with the behavior and intensity of the fire. In contrast, XCH_4 measurements did not offer insights into the fire direction; they solely indicated heightened emissions during the fire event. Filonchyk et al. (2022) conducted a study examining wildfires in the western US during August and September 2020, utilized data from sources like MODIS, Multi-Angle Implementation of Atmospheric Correction (MAIAC), and TROPOMI, along with meteorological information, to assess the wildfires' impact on air quality. The findings indicated a notable deterioration in air quality across Oregon, California, and Washington, with implications extending to neighbouring states, Canada, and the surrounding oceanic regions. Increased concentrations of $PM_{2.5}$ due to smoke aerosols presented health hazards, particularly affecting vulnerable populations. Yılmaz et al. (2023) investigated the intensity and effects of forest fires occurring in the Aegean and Mediterranean Regions of Türkiye in the year 2021. The analysis, conducted using TROPOMI data, demonstrated that the fires were of high and moderate intensity, resulting in significant losses in vegetation cover and leading to the emission of CO into the atmosphere.

In the literature, numerous studies have investigated the correlation between data gathered from the Sentinel-5P satellite by comparing it with ground stations data to test the reliability of TROPOMI data. In the study by Zheng et al. (2019), a robust correlation (R^2 = 0.72) was observed between the NO_2 concentration derived from TROPOMI over a one-year period and the ground-based data obtained from surface monitoring stations. Vîrghileanu et al. (2020), in a certain part of their study, examined the correlation between ground data and NO_2 data obtained from TROPOMI in eight different study areas located in Spain, Germany, the United Kingdom, Italy, and France. According to their findings, the correlation coefficient varied between 0.5 and 0.75, showing differences depending on the study region. Magro et al. (2021) observed and compared TROPOMI-monitored CO and CH_4 levels during forest fires in Portugal with ground stations, revealing a correlation of $R^2 = 0.50$ in their findings. Yılmaz et al. (2023) found correlation coefficients of 0.65 for SO_2 data and 0.83 for NO_2 data between TROPOMI and ground station-based data.

The primary goal of this research is to evaluate the extent of air pollutant gases released during the summer 2021 forest fires in Marmaris and Manavgat, Türkiye. To achieve this objective, the levels of key air pollutants, including CO, NO_2, and aerosols, were examined, utilizing data from the TROPOMI sensor on the Sentinel-5P satellite. In the study, the amounts of CO, NO_2, and aerosol gases released into the air after the fire were compared in three different time periods: (i) the 10-day period before the fire date, (ii) the same fire dates from the previous year, and (iii) the same fire dates from the following year. The Sentinel-2 MSI imagery was utilized to generate Differenced Normalized Burn Ratio (dNBR) maps, which were then used to assess the intensity of the forest fires. This approach aimed to examine the correlation between the severity level of the fires and the investigated air pollutants.

2. METHOD

2.1 Study Areas

The study examines the fires that occurred in approximately the same dates in two regions of Türkiye. The fire regions are located in Marmaris and Manavgat, which are the two districts of the cities Muğla and Antalya, respectively. The locations of fire regions are shown in Figure 1.

Muğla is a South Aegean province, with the majority of its territory in the Aegean Region and a small portion in the Mediterranean Region, having a coastline on both seas. The city of Muğla is influenced by the Mediterranean climate. The "Genuine Mediterranean Climate" is felt in areas up to 800 meters in elevation, while higher elevations experience the "Mediterranean Mountain Climate." The local geographical conditions influence the maximum and minimum temperature values, humidity levels, precipitation amounts, and prevailing wind directions. Muğla, characterized by an annual rainfall exceeding 1000 mm per square meter, stands out as one of the Turkish provinces boasting abundant forest coverage. However, the majority of the precipitation occurs during the winter season, and summer drought is evident (https://mugla.ktb.gov.tr). The lowest and highest temperature reported between 1928 and 2022 in Muğla was -12.1°C and 42.1°C, respectively. The average temperature in this period was 15.2°C (https://www.mgm.gov.tr). In the Marmaris district, summers are notably dry and hot, whereas winters are relatively mild with ample rainfall. Due to the orographic position of the mountains, Marmaris is one of the regions in Türkiye that receives the most precipitation after Rize, and the annual rainfall amount is above 1200 mm (https://www.mugla.bel.tr). The district has a total area of 963.73 km^2, with 80% covered by forested areas and 5% designated for agriculture. It also boasts a coastline length of 451.72 km (http://www.marmaris.gov.tr). The region affected by the fire covers an area of approximately 103.85 km^2.

In Antalya, where the Mediterranean climate prevails, summers are dry and hot, while winters are mild and rainy. With this characteristic, the city falls into the sea and warm sea climate class. In the more inland and mountainous areas of the city, a cold and semi-continental climate type is observed (https://antalya.com.tr). The temperature in Antalya ranged from -4.6°C to 45°C between 1930 and 2022, marking the lowest and highest recorded values (https://www.mgm.gov.tr). Antalya's vegetation consists of maquis, composed of short-statured and evergreen trees throughout the year. The region, rich in forests, is predominantly covered by pine, cedar, and fir forests. In addition to these species, juniper, oak, plane tree, myrtle, laurel, Turkish pine, fir, and olive trees are also encountered (https://antalya.com.tr). Manavgat is the largest district in the Antalya province with an area of 2394 km^2 (http://www.manavgat.gov.tr). The district is situated on the same-named and fertile plain on both sides of the Manavgat River. The district center is approximately 3.5 km away from the Mediterranean coast. Located in the delta of the Manavgat Plain, the district is 75 km east of Antalya and 60 km west of the Alanya district (https://www.matso.org.tr). The region affected by the fire covers an area of approximately 491.41 km^2.

2.2 Data Acquisition

The first Copernicus mission devoted to atmospheric surveillance, the Copernicus Sentinel-5P mission, was launched successfully on October 13, 2017. The primary goal of the Copernicus Sentinel-5P mission is to gather high spatiotemporal resolution atmospheric data for use in air quality, UV and ozone monitoring, and climate forecasting (Veefkind et al., 2012). In the study, satellite data products for determining air pollution, specifically CO, NO_2, and AAI, were obtained from the TROPOMI sensor of the Sentinel-5P (with a spatial resolution of 0.01 arc degrees). To generate dNBR maps, Sentinel-2 MultiSpectral Instrument (MSI) Level-2A imagery (10 m spatial resolution) was used. This imagery offers Surface Reflectance (SR) images that have undergone atmospheric correction, derived from the corresponding Level-1C products (Chaves et

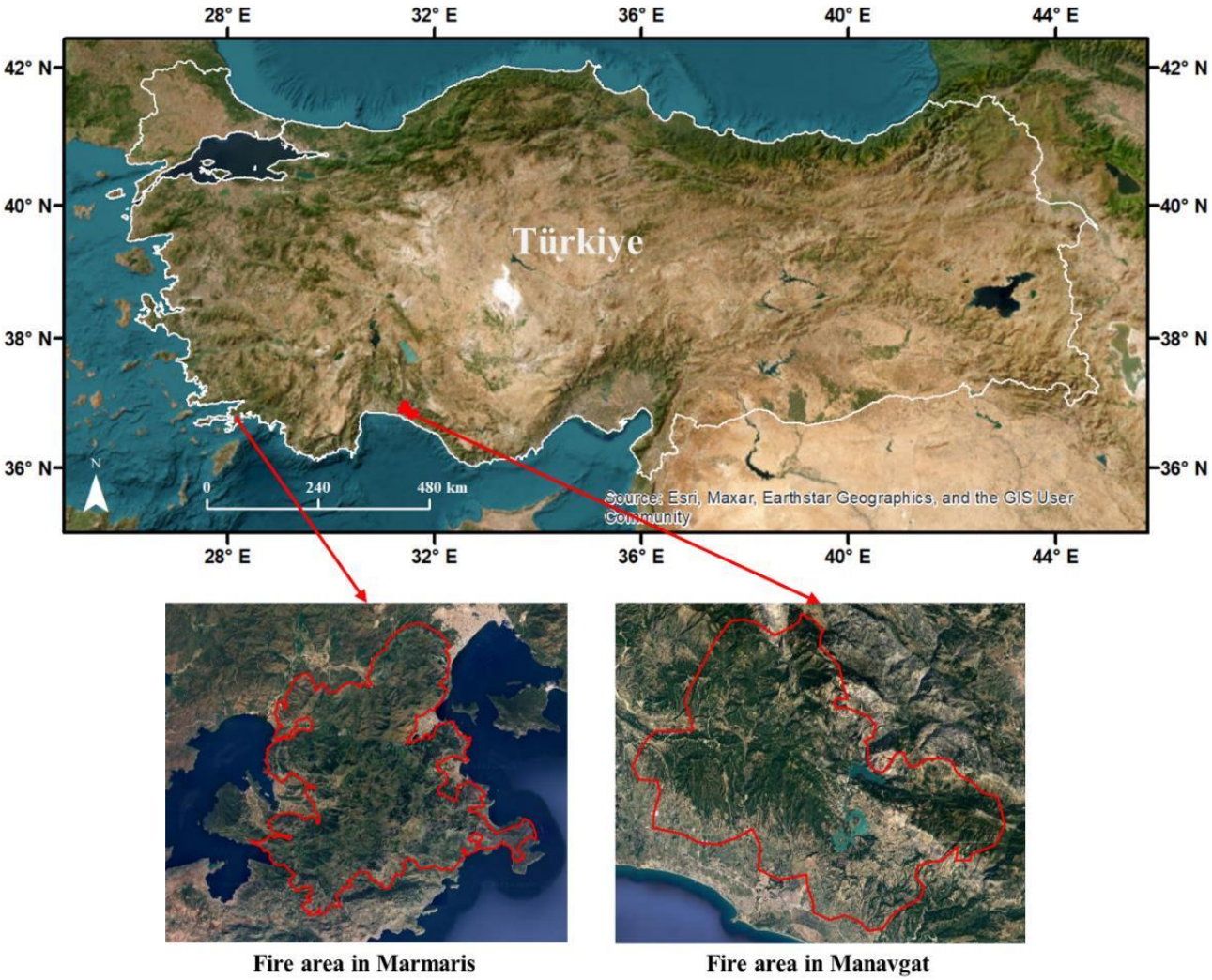

Figure 1. Study Areas.

al., 2020). All the data utilized in the study were sourced from Google Earth Engine (GEE), a cloud-based platform that offers convenient and free access to a wide range of data.

2.3 Emission Data

CO: Carbon monoxide (CO) is a colorless and odorless gas harmful to humans, with a vital role as a trace gas in tropospheric chemistry elucidation (Kleinman, 2020). It acts as a notable atmospheric pollutant in certain urban territories. The main sources of CO encompass fossil fuel combustion, biomass burning, and the atmospheric oxidation of methane. TROPOMI aboard the Sentinel-5P satellite monitors the global concentration of CO by utilizing Earth radiance measurements in the shortwave infrared (SWIR) portion of the spectrum, both in clear-sky and cloudy-sky conditions. The access ID for the CO image collection on the GEE platform is 'COPERNICUS/S5P/NRTI/L3_CO' (https://developers.google.com/earth-engine/datasets/catalog/COPERNICUS_S5P_NRTI_L3_CO).

NO_2: NO_2 is a gas formed as a result of the reaction between nitrogen and oxygen in the atmosphere. Exposure to high concentrations of NO_2 is associated with various respiratory symptoms such as airway inflammation, increased bronchial reactivity, and reductions in immune defense (WHO, 2013; Costa et al., 2014). Nitrogen oxides (NO_2 and NO) are also significant trace gases found in Earth's atmosphere, existing in both the troposphere and the stratosphere. They are introduced into the atmosphere through human activities, particularly the combustion of biomass and fossil fuels, along with natural processes such as wildfires, lightning, and microbiological activities in soils. The image collection ID for NO_2 on the GEE platform is 'COPERNICUS/S5P/NRTI/L3_NO2' (https://developers.google.com/earth-engine/datasets/catalog/COPERNICUS_S5P_NRTI_L3_NO2).

AAI: AAI is a measure used in atmospheric remote sensing to quantify the existance of absorbing aerosols in the Earth's atmosphere. Absorbing aerosols, such as smoke and dust, have the ability to absorb sunlight, affecting the Earth's radiative balance and influencing air quality. The index is responsive to the existance of aerosols that absorb sunlight, such as smoke from wildfires or pollution. The AAI is a unitless measurement parameter, and obtaining a positive value refers to the presence of absorbing aerosols in the atmosphere. The AAI used in the study is provided on the GEE platform with image collection ID 'COPERNICUS/S5P/NRTI/L3_AER_AI' (https://developers.google.com/earth-engine/datasets/catalog/COPERNICUS_S5P_NRTI_L3_AER_AI).

Investigated Periods	Marmaris Start Date-End Date	Manavgat Start Date-End Date
The 10-day period before the fire	19.01.2021-28.01.2021	18.01.2021-27.01.2021
Fire dates	29.07.2021-07.08.2021	28.07.2021-06.08.2021
The same fire dates of the previous year	29.07.2020-07.08.2020	28.07.2020-06.08.2020
The same fire dates of the following year	29.07.2022-07.08.2022	28.07.2022-06.08.2022

Table 1. The details of the investigated periods and corresponding dates.

In the study, the amount of pollutants released during the fire has been compared with three different time periods; (i) the 10-day period before the fire, (ii) the same fire dates of the previous year, (iii) the same fire dates of the following year. The emission data information used in the study are given in Table 1.

2.4 dNBR Mapping

Examining the spatial variations in the intensity of wildfires is crucial for evaluating the ecological and economic impacts and for aligning mitigation strategies. The land surface undergoes damage caused by fire, resulting in some alterations in plant density, water content, and spectral characteristics. This transformation creates suitable conditions for determining the change through spectral bands by causing a modification in the spectral response of the land surface (Lentile et al., 2006; Chuvieco et al., 2006; Robichaud et al., 2007; Boer et al., 2008). For example, Near-Infrared (NIR) bands are sensitive to healthy vegetation. Healthy vegetation reflects a significant amount of light in the NIR region of the spectrum, and this reflectance serves as an indicator of vegetation vigour. On the other hand, SWIR bands are responsive to alterations in the structure and moisture content of vegetation. Burned or stressed vegetation tends to exhibit lower reflectance in the SWIR region. Therefore, Key and Benson (2006) calculated the NBR using these two bands, with the index designed to capture the contrast between the spectral response of healthy vegetation (higher NIR reflectance) and that of burned or stressed vegetation (lower SWIR reflectance). This methodology allows for the detection and assessment of areas affected by fire. The formula for NBR is defined by following equation:

$$NBR = \frac{NIR - SWIR}{NIR + SWIR} \quad (1)$$

In the formula, NIR band in Sentinel-2 images corresponds to Band 8, while the SWIR band is represented by Band 12. The NBR values can range between -1 and 1, with greater values indicating healthier vegetation and lower values associated with burned or stressed vegetation (Key and Benson, 2006).

NBR serves as an assessment of both vegetation health and burn severity, yet it does not inherently reveal temporal changes. Conversely, the dNBR is designed to precisely quantify alterations in burn severity across two distinct time periods. High values of dNBR signify a high degree of severe burn, whereas low and negative values denote lower burn severity and areas that remain unburned. The following equation represents the dNBR formula:

$$dNBR = NBR_{pre} - NBR_{post} \quad (2)$$

In the study, dNBR results were evaluated in five different severity levels as suggested by Key and Benson (2006). See Table 2 for the severity levels considered.

Severity Level	dNBR Values
Unburned	< 0.1
Low	0.1-0.26
Moderate-Low	0.27-0.43
Moderate-High	0.44-0.65
High	≥ 0.66

Table 2. Burn severity levels (Key and Benson, 2006).

In the Marmaris region, dNBR analysis was conducted by averaging Sentinel-2 images for the pre-fire period of '10.07.2021-27.07.2021' and the post-fire period of '01.08.2021-20.08.2021', resulting in 10 m spatial resolution dNBR maps. The time periods for the Manavgat region were determined as the pre-fire period of '08.07.2021-26.07.2021' and the post-fire period of '01.08.2021-20.08.2021'. The Sentinel-2 images were masked with the "QA60" band during the preprocessing stage, but this was not sufficient. Additionally, images were filtered to have a cloud cover rate of less than 10%. Furthermore, a Modified Normalized Difference Water Index (Xu, 2006) was also used as a water mask to eliminate areas containing water features from the images.

3. RESULTS

During the wildfires in Marmaris and Manavgat in the year 2021, there was a significant release of NO_2 and CO into the atmosphere. Detailed information about the gases released into the atmosphere and the amounts of increase for different periods is provided in Table 3. An average of 92.92 μmol/m^2 of NO_2 was emitted into the atmosphere during the fire in Marmaris, showing an increase of 203.63% compared to the 10-day period before the fire, an increase of 204.36% compared to the same fire dates of the previous year, and a 170.16% increase compared to the following year. An average of 0.07 mol/m^2 of CO was released into the air during the same fire, indicating a rise of 102.47% compared to the 10-day period before the fire, a surge of 126.99% compared to the corresponding fire dates from the previous year, and a 126.01% increase compared to the subsequent year. In Figure 2, a time series graph of daily total NO_2 and CO emissions is provided for the year before the fire, the fire year, and the following year. As seen in the figure, there was a significant increase in NO_2 and CO emissions on the 210th day of the year 2021, which corresponds to July 29th, when the Marmaris fire started. The same variation can be observed for the Manavgat fire (see Figure 2).

Marmaris				
Investigated Periods	**NO_2**		**CO**	
	average emission ($\mu mol/m^2$)	increase (%)	average emission (mol/m^2)	increase (%)
Fire dates	92.919	-	0.073	-
The 10-day period before the fire	30.602	203.633	0.036	102.469
The same fire dates of the previous year	30.530	204.356	0.032	126.990
The same fire dates of the following year	34.395	170.156	0.032	126.012
Manavgat				
Investigated Periods	**NO_2**		**CO**	
	average emission ($\mu mol/m^2$)	increase (%)	average emission (mol/m^2)	increase (%)
Fire dates	80.369	-	0.071	-
The 10-day period before the fire	22.298	260.438	0.034	107.071
The same fire dates of the previous year	21.873	267.444	0.031	129.794
The same fire dates of the following year	22.529	256.736	0.031	131.157

Table 3. The emissions of NO_2 and CO in the atmosphere for the examined periods.

Investigated Periods	Marmaris		Manavgat	
	AAI_{min}	AAI_{max}	AAI_{min}	AAI_{max}
Fire dates	-0.125	5.208	0.582	2.953
The 10-day period before the fire	-0.436	0.141	-1.664	0.298
The same fire dates of the previous year	-2.316	-1.844	-1.958	-1.332
The same fire dates of the following year	-1.103	0.128	-0.792	0.005

Table 4. The AAI values for the investigated periods.

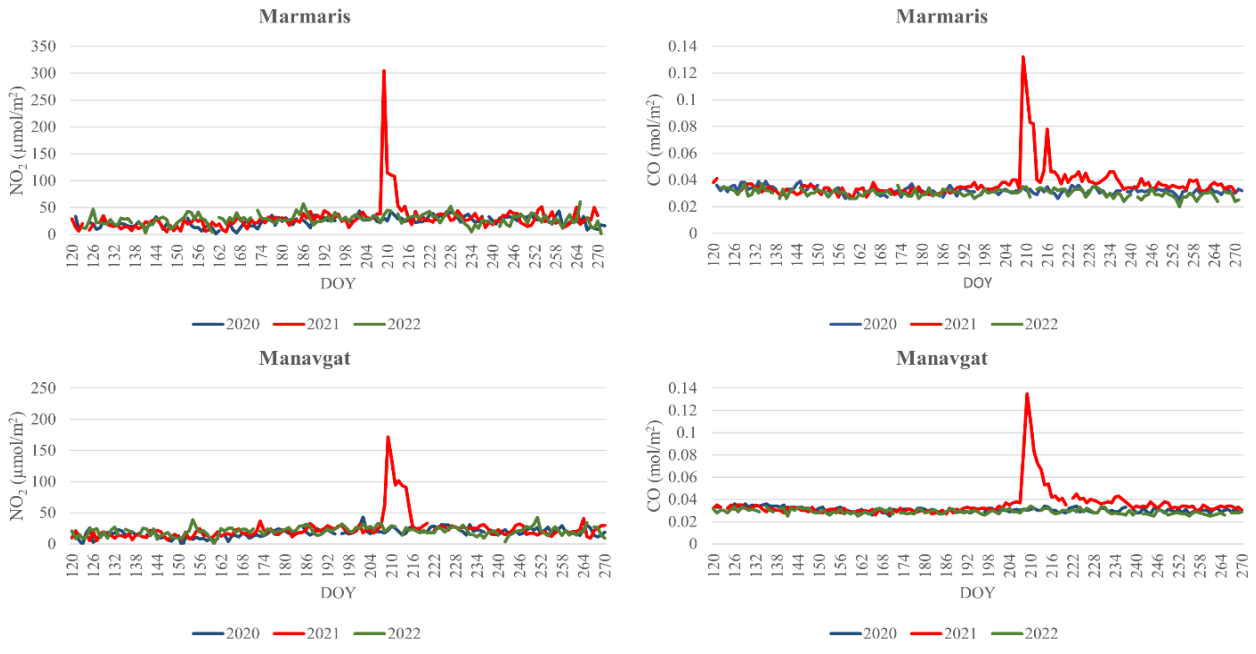

Figure 2. Time series graph of daily total NO_2 and CO emissions in 2020, 2021 and 2022.

Based on the information provided in Table 3, there was an emission of an average of 80.37 $\mu mol/m^2$ of NO_2 into the air during the Manavgat fire. This reflected a surge of 260.44% compared to the 10-day period preceding the fire, an increase of 267.44% compared to the corresponding fire dates of the previous year, and a rise of 256.74% compared to the next year. During the same fire, an average of 0.07 mol/m^2 of CO was emitted into the atmosphere. This indicated a rise of 107.07% compared to 10-day period before fire, an increase of 129.79% compared to the equivalent fire dates of the previous year, and a

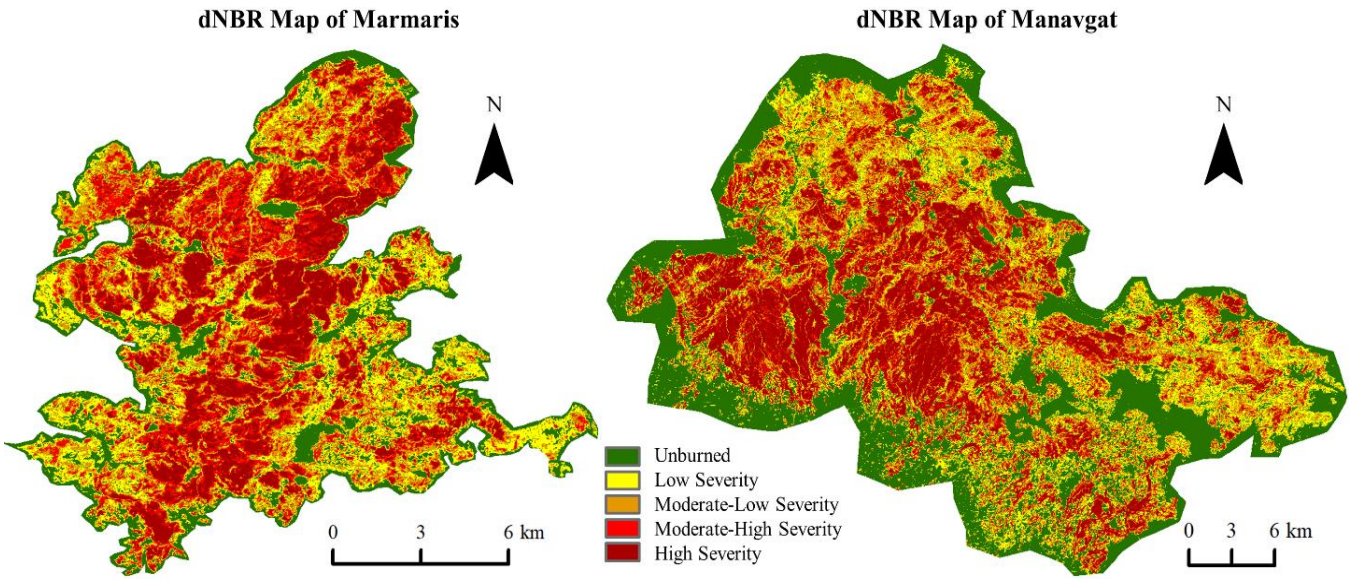

Figure 3. dNBR maps of the fire areas in Marmaris and Manavgat.

surge of 131.16% compared to the following year.

Table 4 displays the calculated AAI values in the atmosphere throughout the examined periods. Positive AAI values indicate the existance of UV-absorbing aerosols in the atmosphere. It is observed that AAI values tend to be positive and high during the wildfire, while during periods outside of the wildfire, they tend to be negative or low.

Table 5 presents the burn severity conditions in Marmaris and Manavgat fire regions. The table depicts that in the Marmaris region, the total impacted area due to the fire encompassed 103.85 km², whereas the completely unaffected area measured 22.57 km². Of the total burned area, 26.84% experienced high severity, 25.01% had moderate-high severity, 25.29% exhibited moderate-low severity, and 22.86% faced low severity of burning. In the Manavgat region, however, an area of 211.18 km² was affected by the fire. The total impacted area due to the fire encompassed 491.41 km², and of this, an area of 122.26 km², corresponding to 24.90%, burned at a high severity. Areas of 107.30 km² and 132.75 km² burned at moderate-high and moderate-low severity levels, respectively. 26.25% of the total area impacted by the fire burned at low severity. Figure 3 shows the dNBR maps of the fire areas in Marmaris and Manavgat to present the spatial distribution of burn severity.

Severity Level	**Area (km²)**	
	Marmaris	**Manavgat**
Unburned	22.57	211.18
Low	23.74	129.00
Moderate-Low	26.26	132.75
Moderate-High	25.98	107.30
High	27.87	122.36
Total Burned	**103.85**	**491.41**

Table 5. Burn severity conditions in Marmaris and Manavgat.

4. DISCUSSION&CONCLUSION

The primary objective of this comprehensive study is to meticulously assess and analyze the voluminous data surrounding air pollutant gas emissions during the extensive forest fires that ravaged Marmaris and Manavgat in Türkiye during the summer of 2021. In pursuit of this goal, an in-depth investigation delving into the concentrations of key air pollutants such as CO, NO_2, and aerosols was conducted. The data harnessed for this endeavor was diligently collected by the cutting-edge TROPOMI sensor on board the Sentinel-5P satellite, providing a wealth of information for a nuanced and detailed analysis.

Upon scrutinizing the results, a glaring pattern emerges, showcasing a staggering increase of over 200% in the release of NO_2 gas during the fire compared to other periods under consideration. This alarming revelation sheds light on the immediate and substantial impact of the forest fires on the atmospheric composition. Furthermore, the analysis discerns that CO gas witnessed an average increase of approximately 120% during the fiery episodes.

A noteworthy finding of the study revolves around the AAI measurements, which unveiled positive and high values in both fire-stricken regions. These observations point to the existance of UV-absorbing aerosols in the atmospheric composition, offering additional layers of insight into the intricacies of the aftermath of forest fires.

The geographical extent of the devastation wrought by the fires was measured, revealing a total affected area of 103.85 km^2 in Marmaris and 491.41 km^2 in Manavgat. Despite the larger spatial footprint of the fires in Manavgat, the quantity of NO_2 released into the atmosphere during the fire was found to be greater in Marmaris. This intriguing dynamic warrants further exploration, emphasizing the need for a multi-dimensional approach to interpreting environmental data.

Furthermore, an intriguing revelation from the analysis is brought to the forefront. Despite significant differences in the fire-affected areas, average CO emissions showed surprising

similarity in both Marmaris and Manavgat throughout the study. This observation prompts further exploration of factors like soil, vegetation, combustible materials, and weather, contributing to the overall complexity of forest fire environmental impact.

In conclusion, this study not only underscores the immediate and substantial influence of forest fires on air quality but also emphasizes the importance of comprehensive, multi-period analyses to glean a more nuanced understanding of the intricate dynamics. The intertwining factors influencing gas emissions necessitate a holistic approach, ensuring a thorough comprehension of the environmental consequences of such catastrophic events.

REFERENCES

Boer, M. M., Macfarlane, C., Norris, J., Sadler, R. J., Wallace, J., Grierson, P. F., 2008: Mapping burned areas and burn severity patterns in SW Australian eucalypt forest using remotely-sensed changes in leaf area index. *Remote Sensing of Environment*, 112(12), 4358-4369.

Brey, S. J., Ruminski, M., Atwood, S. A., Fischer, E. V., 2018: Connecting smoke plumes to sources using Hazard Mapping System (HMS) smoke and fire location data over North America. *Atmospheric Chemistry and Physics*, 18(3), 1745-1761.

Butt E.W., Conibear L., Reddington C.L., Darbyshire E., Morgan W.T., Coe H., Artaxo P., Brito J., Knote C., Spracklen D.V., 2020: Large air quality and human health impacts due to Amazon forest and vegetation fires. *Environmental Research Communications*, 2(9), 095001.

Chaves, M., Picoli, C.A., M., D., Sanches, I., 2020: Recent applications of Landsat 8/OLI and Sentinel-2/MSI for land use and land cover mapping: a systematic review. *Remote Sensing*, 12, 3062.

Chuvieco, E., Riaño, D., Danson, F. M., & Martin, P., 2006: Use of a radiative transfer model to simulate the postfire spectral response to burn severity. *Journal of Geophysical Research: Biogeosciences*, 111(G4).

Costa, S., Ferreira, J., Silveira, C., Costa, C., Lopes, D., Relvas, H., Paulo Teixeira, J., 2014: Integrating health on air quality assessment—review report on health risks of two major European outdoor air pollutants: PM and NO2. *Journal of Toxicology and Environmental Health*, 17(6), 307-340.

FAO, 2022. The State of the World's Forests 2022. Forest pathways for green recovery and building inclusive, resilient and sustainable economies; FAO: Rome, Italy. doi.org/10.4060/cb9360en.

Filonchyk, M., Peterson, M. P., Sun, D., 2022: Deterioration of air quality associated with the 2020 US wildfires. *Science of The Total Environment*, 826, 154103.

GEE, Data Catalog. "Sentinel-5P NRTI CO: Near Real-Time Carbon Monoxide". https://developers.google.com/earth-engine/datasets/catalog/COPERNICUS_S5P_NRTI_L3_CO, (accessed in November 2023).

Ghasempour, F., Sekertekin, A., Kutoglu, S. H., 2021: Google Earth Engine based spatio-temporal analysis of air pollutants before and during the first wave COVID-19 outbreak over Turkey via remote sensing. *Journal of Cleaner Production*, 319, 128599.

Goparaju, L., Pillutla, R. C. P., & Venkata, S. B. K., 2023: Assessment of forest fire emissions in Uttarakhand State, India, using Open Geospatial data and Google Earth Engine. *Environmental Science and Pollution Research*, 30(45), 100873-100891.

Gündüz, H. I., 2018: Uzaktan Algılama ve Coğrafi Bilgi Sistemleri Entegrasyonu ile Aksaray İli Hava Kalitesi Haritasının Oluşturulması, Yüksek Lisans Tezi, Aksaray Üniversitesi Fen Bilimleri Enstitüsü.

Gupta, P., Christopher, S. A., Wang, J., Gehrig, R., Lee, Y. C., Kumar, N., 2006: Satellite remote sensing of particulate matter and air quality assessment over global cities. *Atmospheric Environment*, 40(30), 5880-5892.

Harbula, J., Kopacková, V., 2011. Air pollution detection using MODIS data, *In Earth Resources and Environmental Remote Sensing/GIS Applications II*, SPIE, 8181, 303-317.

Key, C.H., Benson, N.C., 2006: Landscape assessment: sampling and analysis methods. USDA Forest service, rocky mountain research station general technical report RMRS-GTR-164-CD, Ogden.

Kleinman, M. T., 2020: Carbon monoxide. Environmental Toxicants: Human Exposures and Their Health Effects, 455-486.

Lentile, L. B., Holden, Z. A., Smith, A. M., Falkowski, M. J., Hudak, A. T., Morgan, P., Andrew T., Morgan, P., Lewis, S.A., Gessler, P.E., Benson, N.C., 2006: Remote sensing techniques to assess active fire characteristics and post-fire effects. *International Journal of Wildland Fire*, 15(3), 319-345.

Lim, H.S., MatJafri, M.Z., Abdullah, K., Saleh, N.M., AlSultan, S., 2004. Remote sensing of PM10 from Landsat TM imagery. *25th Asian Conference on Remote Sensing*, Thailand, 739-744.

Magro, C., Nunes, L., Gonçalves, O. C., Neng, N. R., Nogueira, J. M., Rego, F. C., Vieira, P., 2021: Atmospheric trends of CO and CH4 from extreme wildfires in Portugal using Sentinel-5P TROPOMI level-2 data. *Fire*, 4(2), 25.

Randerson, J. T., Chen, Y., Van Der Werf, G. R., Rogers, B. M., Morton, D. C., 2012: Global burned area and biomass burning emissions from small fires. *Journal of Geophysical Research: Biogeosciences*, 117(G4).

Retalis, A. 1999: Assessment of the distribution of aerosols in the area of Athens with the use of Landsat Thematic Mapper data, *International Journal of Remote Sensing*, 20(5), 939-945.

Robichaud, P. R., Lewis, S. A., Laes, D. Y., Hudak, A. T., Kokaly, R. F., Zamudio, J. A., 2007: Postfire soil burn severity mapping with hyperspectral image unmixing. *Remote Sensing of Environment*, 108(4), 467-480.

Shmuel, A., Heifetz, E., 2022: Global wildfire susceptibility mapping based on machine learning models. *Forests*, 13(7), 1050.

Sifakis, N., Deschamps, P. Y., 1992: Mapping of air pollution using SPOT satellite data, *Photogrammetric Engineering and Remote Sensing*, 58, 1433-1433.

Tanré, D., Deschamps, P. Y., Devaux, C., Herman, M., 1988: Estimation of Saharan aerosol optical thickness from blurring effects in Thematic Mapper data. *Journal of Geophysical Research: Atmospheres*, 93(D12), 15955-15964.

Tariq, S., ul-Haq, Z., Mariam, A., Mehmood, U., Ahmed, W., 2023: Assessment of air quality during worst wildfires in Mugla and Antalya regions of Turkey. *Natural Hazards*, 115(2), 1235-1254.

Veefkind, J.P., Aben, I., McMullan, K., Förster, H., De Vries, J., Otter, G., Levelt, P.F., 2012: TROPOMI on the ESA Sentinel-5 precursor: a GMES mission for global observations of the atmospheric composition for climate, air quality and ozone layer applications. *Remote Sensing of Environment*, 120, 70–83.

Vîrghileanu, M., Săvulescu, I., Mihai, B. A., Nistor, C., Dobre, R., 2020: Nitrogen Dioxide (NO2) Pollution monitoring with Sentinel-5P satellite imagery over Europe during the coronavirus pandemic outbreak. *Remote Sensing*, 12(21), 3575.

Wald, L., 1999: Observing air quality over the city of Nantes by means of Landsat thermal infrared data, *International Journal of Remote Sensing*, 20(5), 947-959.

WHO, World Health Organization, 2013: Review of evidence on health aspects of air pollution–REVIHAAP project: final technical report. *Bonn: WHO European Centre for Environment and Health*.

Xu, H., 2006: Modification of normalised difference water index (NDWI) to enhance open water features in remotely sensed imagery. *International Journal of Remote Sensing*, 27(14), 3025-3033.

Yilmaz, O. S., Acar, U., Sanli, F. B., Gulgen, F., Ates, A. M., 2023: Mapping burn severity and monitoring CO content in Türkiye's 2021 wildfires, using Sentinel-2 and Sentinel-5P satellite data on the GEE platform. *Earth Science Informatics*, 16(1), 221-240.

Zheng, Z.; Yang, Z.; Wu, Z.; Marinello, F., 2019: Spatial Variation of NO2 and Its Impact Factors in China: An Application of Sentinel-5P Products. *Remote Sensing*, 11, 1939.